remote sensing

MDPI

Communication

Enhanced Pre-STAP Beamforming for Range Ambiguous Clutter Separation with Vertical FDA Radar

Weiwei Wang [1], Pengfei Wan [2], Jun Zhang [2], Zhixin Liu [2] and Jingwei Xu [2,*]

[1] Xi'an Institute of Space Radio Technology, Xi'an 710100, China; tianm1@cast504.com
[2] National Lab of Radar Signal Processing, Xidian University, Xi'an 710071, China; wanpengfei@stu.xidian.edu.cn (P.W.); 21023110391@stu.xidian.edu.cn (J.Z.); zhixinliu@stu.xidian.edu.cn (Z.L.)
* Correspondence: jwxu@xidian.edu.cn

Abstract: Medium pulse repetition frequency (MPRF) is an important mode in airborne radar system. Since MPRF mode brings both Doppler and range ambiguities, it causes difficulty for the airborne radar to suppress ground or sea clutter. In recent years, it has been pointed out that the frequency diverse array (FDA) radar is capable of separating the range ambiguous clutter, which is helpful for the airborne radar in detecting weak moving targets originally buried in ambiguous clutter. To further improve the ambiguous clutter separation performance, an enhanced pre-STAP beamforming for range ambiguous clutter suppression is proposed for the vertical FDA planar array in this paper. With consideration of range dependence of the vertical spatial frequency, a series of pre-STAP beamformers are designed using a priori knowledge of platform and radar parameters. The notches of the beamformers are aligned with the ambiguous clutter to extract echoes from desired range region while suppressing clutter from ambiguous range regions. The notches can be widened by using covariance matrix tapering technique and the proposed method can improve the performance of range ambiguous clutter separation with limited degrees-of-freedom (DOFs). Simulation examples show the effectiveness of the proposed method.

Keywords: airborne radar; range ambiguous clutter; frequency diverse array; pre-STAP beamforming; covariance matrix tapering

Citation: Wang, W.; Wan, P.; Zhang, J.; Liu, Z.; Xu, J. Enhanced Pre-STAP Beamforming for Range Ambiguous Clutter Separation with Vertical FDA Radar. *Remote Sens.* **2021**, *13*, 5145. https://doi.org/10.3390/rs13245145

Received: 28 October 2021
Accepted: 16 December 2021
Published: 18 December 2021

1. Introduction

Space-time adaptive processing (STAP) jointly explores multiple channels and several pulses to discriminate target from clutter and jamming in the spatial-temporal domain, which has found wide applications [1,2]. For the airborne fire-control radar, the Doppler spectrum is widely spread and it is usually impossible to avoid Doppler and range ambiguities simultaneously. To avoid serious Doppler ambiguity due to the widely spread Doppler frequency, medium pulse repetitive frequency (MPRF) is usually adopted in practice. Besides, array radar oriented other than sidelooking will bring up the range dependence problem. In this case, the identical independent distribution (IID) characteristic of the clutter is no longer satisfied, causing adaptive processing performance degradation. More seriously, radar working in MPRF mode usually comes up with the range ambiguity problem which makes the nonstationarity of clutter even worse. In this case, the near-range and far-range regions would be illuminated by the same transmit pulse beam, the corresponding echoes are collected in different pulses but overlapped due to the limited pulse repetition interval. Such coexistence of the range ambiguity and the range dependence causes difficulty in suppression of clutter and detection of moving targets.

It is important for STAP-based radar in non-sidelooking geometry to solve the range ambiguity problem. Many studies have been carried out explore the characteristics in the elevation domain in order to alleviate the range ambiguity problem, such as three-dimensional (3D) STAP method [3,4]. 3D-STAP utilizes elevation diversity to null out

the range-dependent and range-ambiguous clutter; however, this technique increases the system degrees-of-freedom (DOFs) essentially and leverages a really high computational complexity. The azimuth-elevation-Doppler beam is explored for designing a reduced dimension 3D-STAP technique in [5], which addresses the limited training samples and high computational complexity problems. In [6], an efficient method is proposed by transforming the planar array data cube into linear array data matrix, which enables beamforming for an equivalent cross-shaped array before performing STAP procedure. A column subarray synthesis algorithm with pre-filtering in elevation is proposed in [7]. This method tries to use the elevation DOFs to distinguish the echoes from different ranges and to mitigate clutter from the near-range area by using a non-adaptive approach without any increment of STAP computational burden. However, the elevation angles corresponding to the near-range area occupy a large range, thus a lot of DOFs in elevation are needed to suppress the short range clutter.

In recent years, it is pointed out that the frequency diverse array (FDA) radar is capable of separating the range ambiguous clutter, which is helpful for the airborne radar in detection of weak moving targets originally buried in ambiguous clutter. Different from the phased array radar, which provides an angle-dependent transmit beampattern, the FDA can generate a range-angle-time-dependent response by introducing a small frequency increment across adjacent array elements [8–10]. The beampattern properties of FDA radar—as well as its advantages—are thoroughly studied in the literature. In [11], a range-ambiguous clutter suppression technique is proposed based on the range dependence property of beampattern for FDA radar wherein range-ambiguous clutter is suppressed using its 'bent' beampattern. Combined with multiple input multiple output (MIMO) technology, it can provide greater DOFs for space-time-frequency control and has drawn considerable attention from many researchers [12–14]. In FDA-MIMO radar, the transmit waveforms are separated in the receiver, and the time-independent transmit steering vector is obtained. In [15], a range ambiguous clutter suppression approach was introduced with the FDA-STAP radar, where a secondary range dependence compensation (SRDC) approach is proposed to address the range dependence problem. In [16], a range-ambiguous clutter suppression approach was devised, which consists of vertical spatial frequency compensation and pre-STAP beamforming. An enhanced three-dimensional localization (3DL) based adaptive range-angle-Doppler processing method was devised in [17] to reduce the dimension of the processor. An extended element pulse coding technique is employed to suppress the range ambiguous clutter in [18]. The space-time-range dependent property and three-dimensional distribution of clutter are further explored in [19]. Considering the deceptive jamming scenario, an enhanced 3D joint domain localized STAP method is proposed in [20] with application of deceptive jamming pre-whitening in the transmit-receive spatial domain.

In general, an increment of DOF is the basic idea for handling the range ambiguous clutter suppression problem in non-sidelooking array geometry. The planar array provides an elevation dimension which can be utilized to improve the clutter suppression performance. However, it lacks training samples in practical application and it requires large DOFs in elevation to meet the clutter suppression performance. Vertical FDA further increases DOFs in elevation since it incorporates range and angle dependent transmit beampattern. The low sidelobe pre-STAP beamformer in [16] also requires large DOFs to suppress strong near-range clutter. In this paper, we further explore the pre-STAP beamforming method for the vertical FDA radar by using a priori knowledge of platform and radar parameters, including the frequency repetitive frequency, maximum detectable range, height of platform, carrier frequency, array configuration et al. It is possible to construct the power spectrum in elevation frequency domain even before collecting the radar echo. In the sequel, the pre-STAP beamformer can be designed. Therefore, the pre-STAP beamformer can form notches to suppress the range ambiguous clutter with limited DOFs in the elevation dimension. Besides, the covariance matrix tapering is performed to enhance robustness of clutter suppression. This paper is organized as follows. The signal mode

with vertical FDA radar is provided in Section 2. In Section 3, the range ambiguous clutter suppression with vertical FDA is briefly outlined and the proposed enhanced pre-STAP beamforming is presented. Simulation results are used to validate the effectiveness of the proposed method in Section 4. Finally, conclusions are drawn in Section 5.

2. Signal Model of Vertical FDA Radar

As shown in Figure 1, a right-hand coordinate is established and an airborne forward-looking array radar system is considered. The height of the platform is H with a velocity denoted by V. A plane array is considered with its column and row numbers are N and M, respectively. The inter space of these elements is d for both column and row. A total of K pulses are transmitted during a coherent processing interval (CPI) with the pulse repetition frequency (PRF) denoted by $f_r = 1/T_r$. L range cells are collected by the radar receiver. The carrier frequency of the Vertical FDA is written as

$$f_m = f_0 + (m-1)\Delta f, m = 1, 2, \cdots, M \tag{1}$$

where f_0 is the reference carrier frequency, Δf is the step frequency which can be much smaller compared with bandwidth of the transmitted baseband signal [12].

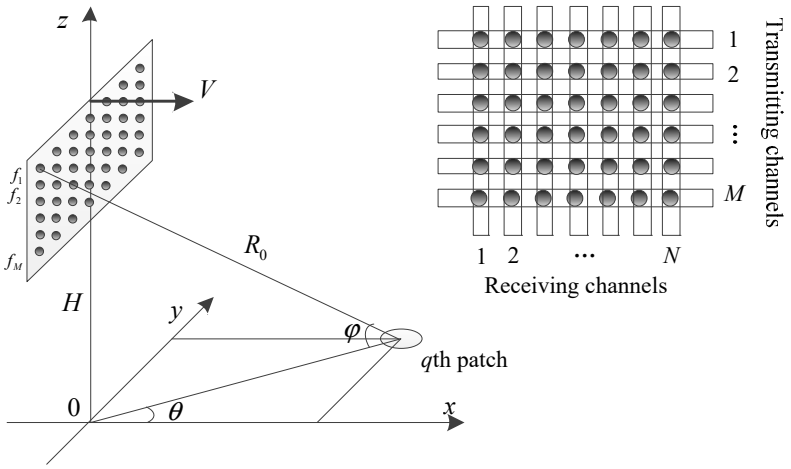

Figure 1. Forward-looking array geometry of airborne radar.

It is assumed that each row transmits orthogonal waveform [16]; thus, it seems like there are M transmitting channels whose equivalent phase centers are at the midpoints of the corresponding rows. In the receive chain, the measured signals are down converted, matched filtered, and stored. It can be interpreted as there are N receiving channels whose equivalent phase centers are the midpoints of columns. Therefore, the array structure can be viewed as M transmitters and N receivers. The narrowband assumption is used in this paper and we choose the most left-upper element as the reference point. The ground clutter return corresponding to the lth range cell results from the coherent summation of the many scattering centers within the bounds of each iso-range, including range ambiguities. Thus, the echo at the kth pulse received by the nth receiver and transmitted by the mth transmitter can be expressed as

$$r_{m,n,k} \approx \sum_{p=1}^{N_a} \sum_{q=1}^{N_c} \xi^{\{p,q\}} \exp\left\{-j2\pi f_m \left(\tau_T^{\{p,q\}} + \tau_R^{\{p,q\}}\right)\right\} \exp\{j2\pi f_d (k-1)T\} \tag{2}$$

where we assume each iso-range (range cell) consists of N_c statistically independent clutter patches, N_a indicates the number of ambiguous ranges. $\xi^{\{p,q\}}$ denotes the radar cross section and p is the number of ambiguous range region while q indicates the qth patch at such range cell. $f_d = \frac{2V}{c} f_0 \cos\theta \cos\varphi$ is the Doppler frequency with θ and φ being the

azimuth angle and elevation angle, respectively. $\tau_T^{\{p,q\}}$ and $\tau_R^{\{p,q\}}$ are the transmitting delay and receiving delay, respectively.

$$\begin{aligned}\tau_T^{\{p,q\}} &= \frac{1}{c}\left(R_0 - \frac{N-1}{2}d\sin\theta\cos\varphi - (m-1)d\sin\varphi\right)\\ \tau_R^{\{p,q\}} &= \frac{1}{c}\left(R_0 - \frac{M-1}{2}d\sin\varphi - (n-1)d\sin\theta\cos\varphi\right)\end{aligned} \tag{3}$$

In the following, we neglect the superscript $\{p, q\}$ in this paper for the sake of simplicity. Consider the narrowband condition and use some mathematic approximation, it yields [16]

$$r_{m,n,k} \approx \sum_{p=1}^{N_a}\sum_{q=1}^{N_c}\xi\exp\{j2\pi(f_R+f_e)(m-1)\}\exp\{j2\pi f_a(n-1)\}\exp\{j2\pi f_t(k-1)\} \tag{4}$$

where f_R, f_e, f_s, and f_t are the normalized range frequency, elevation frequency, azimuth frequency, and normalized Doppler frequency—i.e., $f_e = \Delta f\frac{2R_0}{c}$, $f_e = \frac{d}{c}f_0\sin\varphi$, $f_a = \frac{d}{c}f_0\sin\theta\cos\varphi$, and $f_t = \frac{2VT}{c}f_0\cos\theta\cos\varphi$, respectively. It is noted that Equations (2) and (4) are obtained with reasonable simplification by ignoring the second-order phase terms with respect to transmit element number, as the freuqency increment is neglegible compared with the carrier frequency. Thus, an effective model for the clutter elevation-azimuth-time three-dimensional snapshot takes the form of

$$\boldsymbol{c}_l = \sum_{p=1}^{N_a}\sum_{q=1}^{N_c}\xi\boldsymbol{s}_t\otimes\boldsymbol{s}_a\otimes\boldsymbol{s}_e \tag{5}$$

where $\otimes$ is the kronecker product, the subscript l indicates the lth range cell. $\boldsymbol{s}_t\in C^{K\times 1}$, $\boldsymbol{s}_a\in C^{N\times 1}$, and $\boldsymbol{s}_e\in C^{M\times 1}$ are the corresponding time steering vector, azimuth steering vector, and elevation steering vector.

$$\boldsymbol{s}_t = [1,\exp\{j2\pi f_t\},\cdots,\exp\{j2\pi f_t(K-1)\}]^{\mathrm{T}} \tag{6}$$

$$\boldsymbol{s}_a = [1,\exp\{j2\pi f_a\},\cdots,\exp\{j2\pi f_a(N-1)\}]^{\mathrm{T}} \tag{7}$$

$$\boldsymbol{s}_e = [1,\exp\{j2\pi(f_R+f_e)\},\cdots,\exp\{j2\pi(f_R+f_e)(M-1)\}]^{\mathrm{T}} \tag{8}$$

The obtained echo $\boldsymbol{c}_l$ is an MNK dimensional vector in the transmit, receive, and Doppler dimensions. Because of the difference of the carrier frequencies, the data snapshot in (5) is slightly different from that of the traditional 3D-STAP [3]. However, it is right that the difference provides extra information to mitigate the range-ambiguous clutter. In the following section, the characteristics in the elevation frequency domain are further explored and a range-ambiguous clutter suppression method is proposed.

3. Range-Ambiguous Clutter Suppression Based on Pre-STAP Beamforming Method

In this section, the characteristic of the FDA in elevation is analyzed. Compared with the elevation frequency spectrum of the traditional phased array, that of FDA can be widely spread in the elevation frequency domain, thus clutter from different range rings can be extracted respectively. For the traditional phased array radar, the elevation frequency is monotonically decreasing with respect to the slant range. It is a sinusoidal function with respect to the elevation angle, and it changes slowly and slowly with the increase of slant range. In contrast, the characteristic of the elevation frequency in the FDA radar will allow us to separate the range-ambiguous clutter easier. As shown in (8), the elevation steering vector can be viewed as a narrow-band signal impinging on the array with equivalent elevation frequency being the sum of f_e and f_R. Thus, the overall elevation frequency corresponding to the mth transmitter can be expressed as

$$f_{e\text{-}FDA} = f_R + f_e = \frac{\Delta f}{c}2R_0 + \frac{d}{\lambda_0}\sin\varphi = \frac{\Delta f}{c}2R_0 + \frac{d}{\lambda_0}\frac{H}{R_0} \tag{9}$$

where $f_{e\text{-}FDA}$ denotes the elevation frequency of vertical FDA radar. As shown in (9), the elevation frequency differs from that of the traditional phased array by the range frequency. Consider the range ambiguity case, for the lth range cell and pth range ring, the elevation frequency can be rewritten as

$$f_{e\text{-}FDA} = \frac{\Delta f}{c} 2(R_l + pR_u) + \frac{d}{\lambda_0}\frac{H}{R_0} = \frac{\Delta f}{c} 2R_l + \frac{\Delta f}{c} 2(p-1)R_u + \frac{d}{\lambda_0}\frac{H}{R_0} \tag{10}$$

where $R_0 = R_l + (p-1)R_u$, R_l is the unambiguous slant range for lth range cell and R_u is the ambiguous range, i.e., $R_u = c/2f_r$ and f_r is the pulse repetition frequency. $p = 1,2,\ldots,N_a$ indicates the number of range ring. Thus, f_R is decomposed into two items: the first item is range-dependent and the second item is dependent on the number of range ring. It is seen that the elevation frequency changes greatly due to the linearly increased f_R. As the unambiguous range R_l and the step frequency Δf are known exactly, compensation can be done by using the constructed compensation vector which is expressed as

$$\boldsymbol{h_c}(R_l) = \left[1, \exp\left\{j4\pi\frac{\Delta f}{c}R_l\right\}, \cdots, \exp\left\{j4\pi\frac{\Delta f}{c}R_l(M-1)\right\}\right]^{\mathrm{T}} \tag{11}$$

The elevation-azimuth-time three-dimensional snapshot is compensated at every range cell. The compensation range frequency is written as $\hat{f}_{Rc} = \frac{2\Delta f}{c}R_l$. Therefore, it is required to compute the compensation vectors off-line. In the sequel, the clutter data can be expressed as

$$\widetilde{\boldsymbol{c}}_l = (\boldsymbol{I}_{NK} \otimes \mathrm{diag}\{\boldsymbol{h_c}(R_l)\})\boldsymbol{c}_l = \sum_{p=1}^{N_a}\sum_{q=1}^{N_c} \xi \boldsymbol{s}_t \otimes \boldsymbol{s}_a \otimes (\mathrm{diag}\{\boldsymbol{h_c}(R_l)\}\boldsymbol{s}_e) \tag{12}$$

where $\mathrm{diag}\{\boldsymbol{a}\}$ is a digonal matrix with its entries from the vector $\boldsymbol{a}$, the $\boldsymbol{I}_{NK}$ is an NK-dimenional identity matrix. It is noted that the compensated clutter echo is still an MNK-dimentional vector. Now the corresponding elevation frequency can be written as

$$\hat{f}_{e\text{-}FDA} \approx \frac{\Delta f}{c} 2(p-1)R_u + \frac{d}{\lambda_0}\frac{H}{R_0} = \frac{\Delta f}{f_r}(p-1) + \frac{d}{\lambda_0}\frac{H}{R_0} \tag{13}$$

The elevation frequency is finally expressed as sum of two items: the first item is a function of the number of range ring and the second item is the same as that of the traditional phased array. In Figure 2, the normalized elevation frequency as stated in (13) is shown. Due to the range ambiguity, the elevation frequency can be viewed as a shifted of the traditional elevation frequency $f_{e\text{-}PA}$ with a factor corresponding to the number of range ring. As aforementioned, the elevation frequency spectrum for the traditional phase array radar is band-limited and occupies the positive half range of the normalized frequency axis—i.e., $f_{e\text{-}PA} \in (0, 0.5)$. While for the vertical FDA radar, the elevation frequency spectrum occupies the whole normalized digital frequency range. In other words, as the elevation frequency can be shifted to the negative semi-axis of the normalized frequency axis—i.e., $-0.5 < f < 0$—the range-ambiguous clutter can be widely separated in elevation frequency domain.

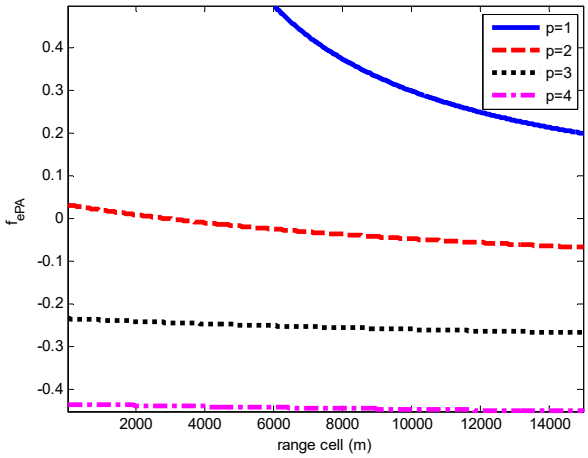

Figure 2. Elevation frequency for FDA radar after compensation.

Because the range ambiguous clutter are widely separated in the vertical frequency domain, it is possible to extract the echoes of desired range regions by using several pre-STAP filters. In [16], the filters in elevation are designed with their coefficients expressed as $\boldsymbol{g}_p = (g_1, g_2, \cdots, g_M)^{\mathrm{T}}$, p = 1,2, ... ,N_a indicates the index of range region. The clutter snapshot can be transformed into an NK-dimensional space-time snapshot as

$$\begin{aligned} \hat{\boldsymbol{c}}_l(p_0) &= \left(\boldsymbol{I}_{NK} \otimes \boldsymbol{g}_{p_0}\right)^{\mathrm{H}} \widetilde{\boldsymbol{c}}_l = \left(\boldsymbol{I}_{NK} \otimes \boldsymbol{g}_{p_0}\right)^{\mathrm{H}} (\boldsymbol{I}_{NK} \otimes \mathrm{diag}\{\boldsymbol{h}_{\boldsymbol{c}}(R_l)\})\boldsymbol{c}_l \\ &= \sum_{p=1}^{N_a} \sum_{q=1}^{N_c} \xi^{\{p,q\}} \left(\boldsymbol{g}_{p_0}^{\mathrm{H}} \mathrm{diag}\{\boldsymbol{h}_{\boldsymbol{c}}(R_l)\}\boldsymbol{s}_e\right)(\boldsymbol{s}_t \otimes \boldsymbol{s}_s) \end{aligned} \tag{14}$$

Here, after the pre-STAP beamformer, the clutter echo is NK-dimensional. In order words, the pre-STAP beamformer is performed in the elevation frequency domain and the output is synthesized with the beamformer. For example, for the first range region, the desired pre-STAP beamformer is indicated as $\boldsymbol{g}_1$, which can be designed with the conventional FIR filters design method. Similarly, the pth ambiguous range ring can be extracted and the clutter spectrum compensation can be done without the bother of the range ambiguity. The echo in the joint azimuth and Doppler domain can be expressed as

$$\hat{\boldsymbol{c}}_l(p_0) = \sum_{q=1}^{N_c} A_{p_0,l} \xi^{\{p_0,q\}} (\boldsymbol{s}_t \otimes \boldsymbol{s}_s) + \sum_{p=1, p\neq p_0}^{N_a} \sum_{q=1}^{N_c} A_{p,l} \xi^{\{p,q\}} (\boldsymbol{s}_t \otimes \boldsymbol{s}_s) \tag{15}$$

where $A_{p_0,l}$ is the beamforming output corresponding to the desired range region while $A_{p,l}, p \neq p_0$ denotes the beamforming output corresponding to the non-desired range ambiguous regions. With proper design of the pre-STAP beamformer, it is possible to mitigate the range ambiguous echoes. It is also observed that the passband of the filter corresponding to the first range region is relatively wide. This induces performance degradation for the clutter separation. In this paper, we present an enhanced pre-STAP beamforming method, which incorporates the adaptive digital beamforming theory to null out the nuisance range ambiguous clutter. The vertical beampattern can be designed as

$$\min_{\boldsymbol{g}} \max_{\phi} W(\phi) |P(\phi) - P_d(\phi)| \tag{16}$$

where $W(\phi)$ is the weighting function defined in vertical frequency domain. Here, we design this weighting function with empirical rules: (i) using small weighting scales for the transitional region, and (ii) using larger weighting scales for sidelobe region compared with main lobe region. $P(\phi)$ is the vertical beampattern which can be expressed as

$$P(\phi) = \boldsymbol{g}^H \boldsymbol{a}(\phi) = \sum_{m=1}^{M} g_m^* a_m(\phi) = \sum_{m=1}^{M} g_m^* [\mathrm{diag}\{\boldsymbol{h_c}(R_l)\}\boldsymbol{s}_e]_m = \sum_{m=1}^{M} g_m^* \exp\left\{j2\pi \hat{f}_{e\text{-}FDA}(m-1)\right\} \quad (17)$$

where $[\cdot]_m$ denotes the m-th entry of a vector, $\boldsymbol{g} = (g_1, g_2, \cdots, g_M)^{\mathrm{T}} \in \mathbb{C}^{M\times 1}$ is the vertical weight vector, and $\boldsymbol{a}(\phi)$ is defined as the compensated vertical spatial steering vector which can be written as

$$\boldsymbol{a}(\phi) = \mathrm{diag}\{\boldsymbol{h_c}(R_l)\}\boldsymbol{s}_e = \left[1, \exp\left\{j2\pi \hat{f}_{e\text{-}FDA}\right\}, \cdots, \exp\left\{j2\pi \hat{f}_{e\text{-}FDA}(M-1)\right\}\right] \quad (18)$$

Therefore, the problem of clutter separation is transformed into a pre-STAP beamforming problem with the purpose to suppress range ambiguous clutter effectively. Generally, the low sidelobe property of the vertical beampattern is desirable—i.e., $P_d(\phi)$ have low sidelobe as well as flat-top properties. However, it requires a great number of DOFs, which might not be available in practical applications [16]. Here, we further propose an enhanced pre-STAP beamforming method by incorporating the adapted beampattern design theory. The beampattern is formulated as

$$\min_{\boldsymbol{g}} \boldsymbol{g}^H \boldsymbol{R}_{l,-p_0} \boldsymbol{g} \quad s.t. \begin{cases} \boldsymbol{g}^H \boldsymbol{a}\left(\phi_{l,p}\right) = 1, p = p_0 \\ \boldsymbol{g}^H \boldsymbol{a}\left(\phi_{l,p}\right) = 0, p \neq p_0 \end{cases} \quad (19)$$

where $\boldsymbol{R}_{l,-p_0}$ is the covariance matrix corresponding to l-th range bin but excluding that of the desired range region—that is, $\boldsymbol{R}_{l,-p_0} = \sum_{p=1,p\neq p_0}^{N_a} \boldsymbol{R}_{l,p}$—where p_0 is the desired range region. With the prior knowledge of the airborne radar parameters, the clutter spectrum in vertical frequency domain can be predicted. The objective function in (19) tries to minimize the echo power corresponding to the non-desired range regions. It is seen that the constraints in (19) maintain the echo of the desired range region and mitigate those of the ambiguous range regions. With the minimum variance distortionless response criterion, the enhanced pre-STAP beamformer is obtained. Furthermore, the covariance matrix $\boldsymbol{R}_{l,-p_0}$ is used to further improve the robustness with matrix tapering technique employed, because there are inevitable errors—such as array calibration error, compensation induced error, and so on. The covariance matrix is constructed as

$$\boldsymbol{R}_{l,-p_0} = \sum_{i,p\neq p_0} \xi_p^2 \boldsymbol{a}\left(\phi_{i,p}\right) \boldsymbol{a}^H\left(\phi_{i,p}\right) \quad (20)$$

where ξ_p^2 stands for the power estimation which is obtained by radar equation, $\phi_{i,p}$ is within a small set centered by the equivalent vertical frequency of the l-th range bin and p-th range region—i.e., $\left|\phi_{i,p} - \phi_{l,p}\right| \leq \varepsilon$ with ε controlling the size of set. Note that the covariance matrix can be computed from the known radar parameters and corresponding geometry parameters—including the frequency repetitive frequency, maximum detectable range, height of platform, carrier frequency, array configuration, etc. In the sequel, we further employ a tapering matrix on the covariance matrix [21,22], that is,

$$\widetilde{\boldsymbol{R}}_{l,-p_0} = \boldsymbol{T} \odot \boldsymbol{R}_{l,-p_0} \quad (21)$$

where the tapering matrix $\boldsymbol{T}$ is constructed as

$$[\boldsymbol{T}]_{m,n} = \frac{\sin(|m-n|\xi)}{|m-n|\xi} \quad (22)$$

where ξ is the tapering coefficient controlling the tradeoff between the null depth and the null width. Based on Schur theory, $\widetilde{\boldsymbol{R}}_{l,-p_0}$ is positive semidefinite if $\boldsymbol{T}$ and $\boldsymbol{R}_{l,-p_0}$ are positive semidefinite [23,24].

4. Simulation Examples

In this section, we use simulated data to demonstrate the effectiveness and the superiority of the proposed approach for range-ambiguous clutter mitigation. The planar array is considered and an equivalent cross-shaped array is obtained as aforementioned in Section 2. The simulation parameters are listed in Table 1. The CNR is usually 50–70 dB for the airborne warning radar in scenarios of ground clutter and the CNR is about 30–50 dB in scenarios of sea clutter. In this paper, we use CNR = 40 dB.

Table 1. Simulation parameters.

Parameters	Value	Parameters	Value
Reference carrier frequency	5 GHz	Element distance	0.03 m
Platform velocity	100 m/s	Azimuth channel number	10
Platform height	6000 m	Elevation channel number	10
Pulse repetition frequency	5 kHz	Number of pulses	16
Maximum slant range of clutter	120 km	Clutter-to-noise ratio	50 dB

4.1. Range-Ambiguous Clutter Spectrum

In Figure 3, the range ambiguous clutter spectrum is presented for a forward-looking airborne radar system. The clutter spectrum corresponding to a single range bin is plotted in Figure 3a while the clutter spectrum of all range bins is plotted in Figure 3b. In this simulation, as the unambiguous range is equal to 30 km and the maximum slant range of clutter is 120 km, the range ambiguity number is 4. We consider the ground clutter with the surface covered by woods in the example. As we can see from Figure 3a, clutter spectrum corresponding to the first range region is obviously different from those corresponding to the other range regions, because the range dependence is severe within the near-range area while it becomes slighter in the far-range area. Therefore, clutter from the second, third, and fourth range regions are almost overlapped in the spatial-temporal frequency domain. Here Monto Carlo number is set as 300 and this is only meaningful in theory. In practice, the covariance matrix is estimated with maximum likelihood (ML) criterion by using the training data collected from all the ranges. The clutter spectrum in spatial-temporal domain is shown in Figure 3b, which is spread severely in the right-half space of spatial-temporal domain. Here we use echoes of all range bins as training data, so the range dependence can be obviously observed. It is emphasized that the spreading of Doppler frequency increases the complexity and the range dependency problem. In such case, it is predicted that the slowly-moving target will be buried in the clutter even after STAP procedure.

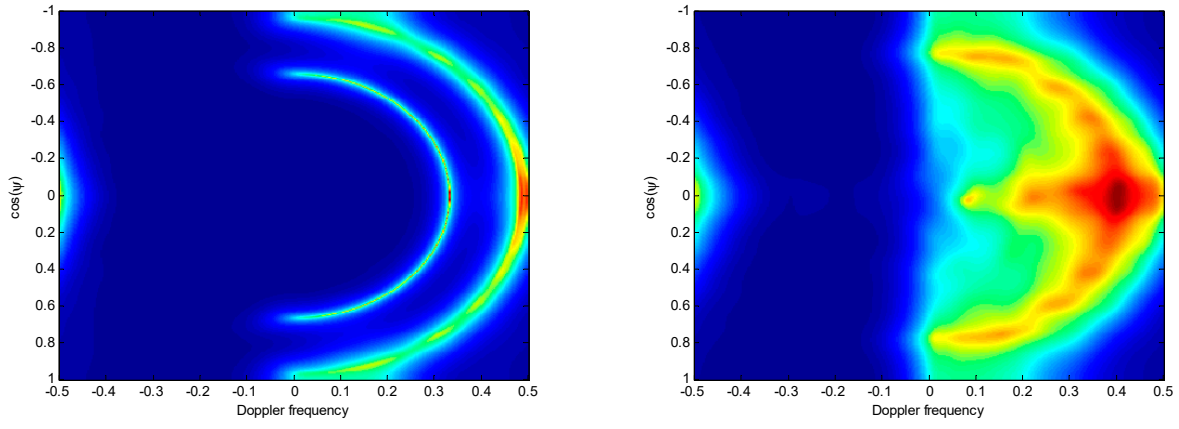

(**a**) (**b**)

Figure 3. Range ambiguous clutter spectrum in spatial-temporal domain: (**a**) a single range cell; (**b**) all slant range cells.

4.2. Clutter Spectrum in Elevation Frequency Domain

Figure 4 shows the clutter spectrum in elevation frequency domain of vertical-FDA radar with its parameters defined in Table 1. Because of the frequency diversity, the elevation frequency changes evidently for all the slant ranges, as stated by (9). The range cell size is 15 m and there are 1000 range bins within the whole unambiguous range. Notice that the data samples in azimuth and pulse dimensions are taken as training samples. Thus, there are sufficient IID training samples. It is seen that the elevation frequency is approximately linearly increasing with respect to slant range for the second, third, and fourth range regions. Therefore, we can say that the range-ambiguous clutter can be separated range by range. With further range dependence compensation process, the clutter spectrum after compensation change slightly with respect to the slant range for the second, third, and fourth range regions. Due to the introduction of frequency diversity, the clutter spectra corresponding to different range regions are still definitely separated. Notice that the clutter spectrum corresponding to first range region still changes greatly with respect to slant range. This is because the sinusoidal function varies evidently in the near range. We also observe that there is no clutter spectrum corresponding to 0 to 6 km because the height of the platform is 6 km. To separate clutter from different range regions in elevation frequency domain, we should treat the first range region different from the other regions.

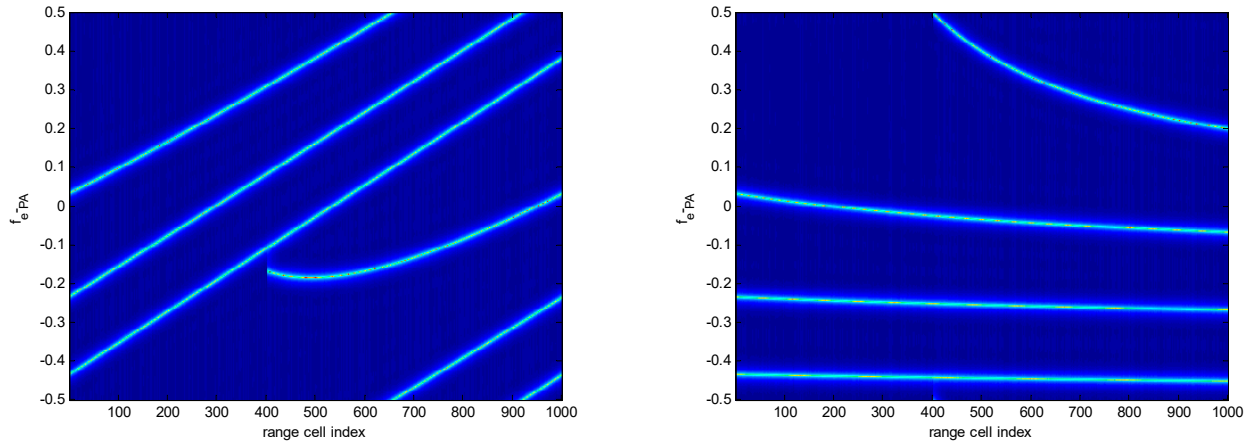

Figure 4. Clutter spectrum in elevation-range domain for FDA radar: (**a**) Before compensation; (**b**) After compensation.

4.3. Pre-STAP Beamformer Response and Range-Ambiguous Clutter Separation

In this subsection, we discuss the pre-STAP beamformer with respect to range. Figure 5a,b plot the basic pre-STAP beamformer and the enhanced pre-STAP beamformer corresponding to the first range region, respectively. The enhanced beamformer is obtained by using covariance matrix tapering. The height of airplane is 6 km and thus there is no clutter echo within 0–6 km, because the vertical frequency varies evidently with respect to range in the first range region. When we need to extract the echoes of the first range region, the main lobe of the beamformer should varies with respect to range. It is seen that the range ambiguous clutter of second, third, and fourth range regions can be sufficiently suppressed since the notches of the beamformer align with the range ambiguous clutter. Moreover, for the enhanced beamformer, the notches are obviously widened which increases the robustness of the beamformer. In this situation, the range ambiguous clutter can always be suppressed even their vertical frequencies are mismatched with presumed ones due to errors. With the prior knowledge of platform and radar system parameters, the pre-STAP beamformer is designed. However, the parameters have errors due to kinds of factors, thus the enhanced beamformer is required in applications. Figure 5c,d plot the basic

beamformer and the enhanced beamformer corresponding to the second range region. It is seen that the notch corresponding to the first range region varies obviously with respect to the range. In contrast, the vertical frequency of main lobe is almost unchanged within the range region.

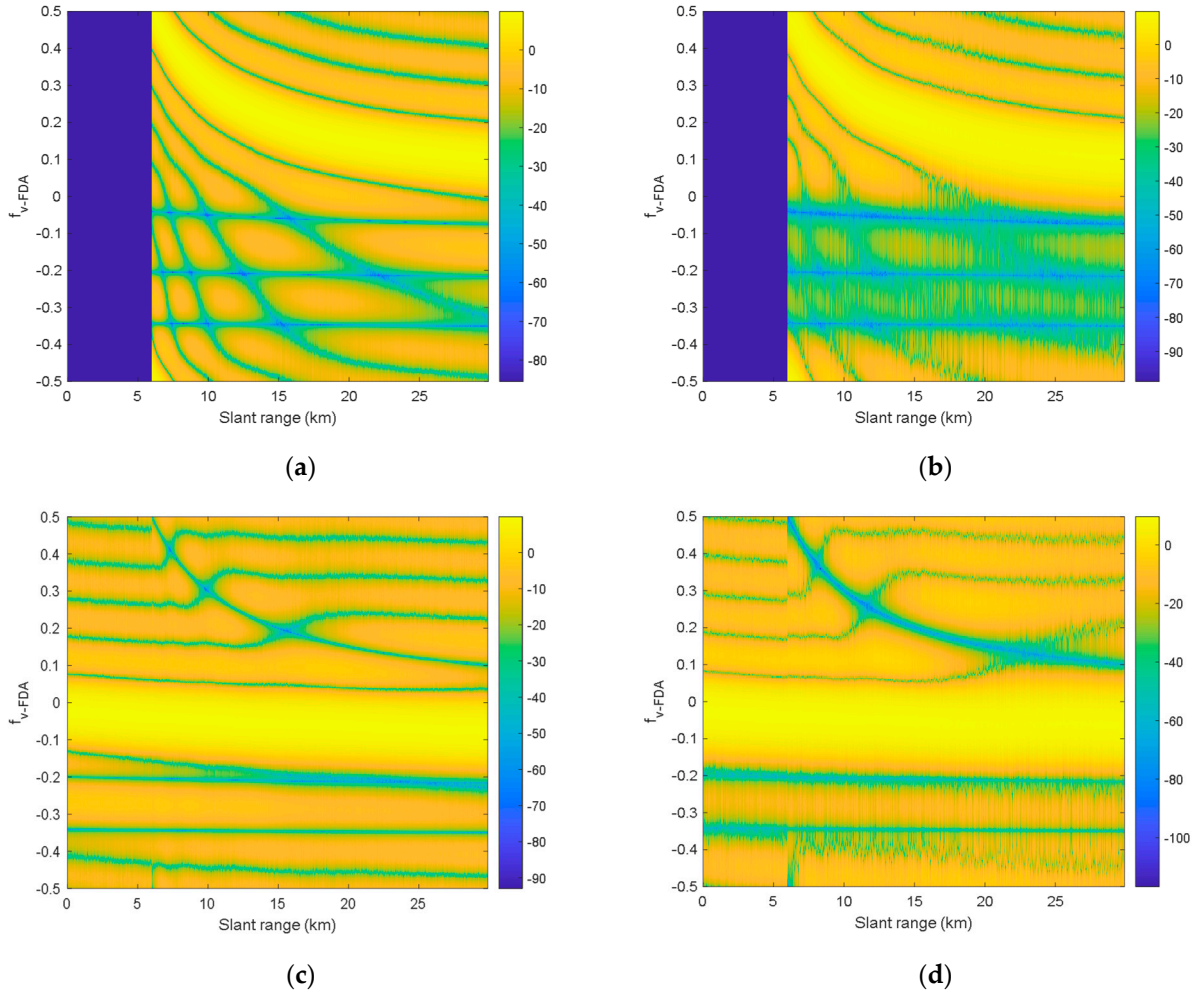

Figure 5. Pre-STAP beamformer with respect to range: (**a**) Pre-STAP beamformer for first range region; (**b**) Enhanced pre-STAP beamformer for first range region; (**c**) Pre-STAP beamformer for second range region; (**d**) Enhanced pre-STAP beamformer for second range region.

Figure 6 presents the beamformer corresponding to a given particular range bin. In this simulation, the range bin index is 1000 and the unambiguous slant range is 15,000 m. The selected range bin in this example is 1000. The original notches of the basic pre-STAP beamformer and the widened notches of the enhanced pre-STAP beamformer are shown as comparison. Besides, the width of notches can be adjusted using the tapering control parameter. In this example, the parameter is set as $\xi = 0.1$ for the tapering matrix in (22). Figure 6a plots the beampatterns of basic and enhanced pre-STAP beamformers corresponding to the first range region while Figure 6b shows the results corresponding to the second range region. By using the designed pre-STAP beamformer, the required DOFs in elevation can be effectively reduced. It is seen that 10 elements in elevation can form notches to suppress the range ambiguous clutter.

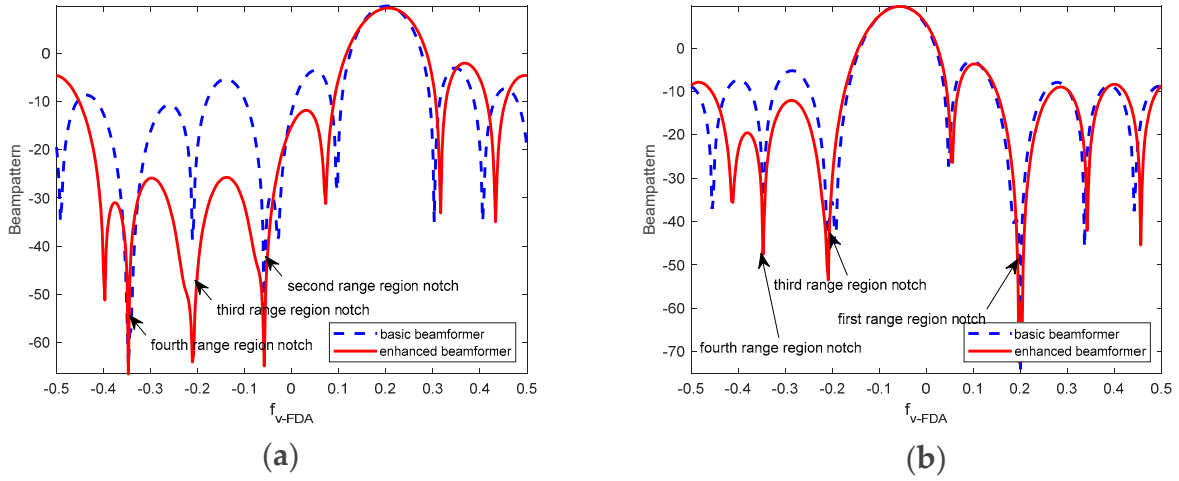

Figure 6. Pre-STAP beamformer for a given range bin: (**a**) First range region; (**b**) Second range region.

In Figure 7, we show the separated range-ambiguous clutter of the first and second range regions to verify the effectiveness of the proposed method. As we can see from these figures, clutter of each range region is successfully separated and thus target detection can be implemented for each range region separately. Specifically, the clutter from the first range region is severely range-dependent and the IID condition is seriously violated, as shown in Figure 7a. The clutter from the second, third, and fourth range regions approximately satisfy the IID condition; thus, STAP can be directly implemented. Here we show the clutter spectrum corresponding to the second range region in Figure 7b. The clutter spectrum is well focused even before applying the clutter compensation technique. It is known that the variance of elevation frequency is rapid and the range dependency problem is severe for the first range ring, while the variance of elevation frequency is slight and the range dependency problem is mild for the other range regions.

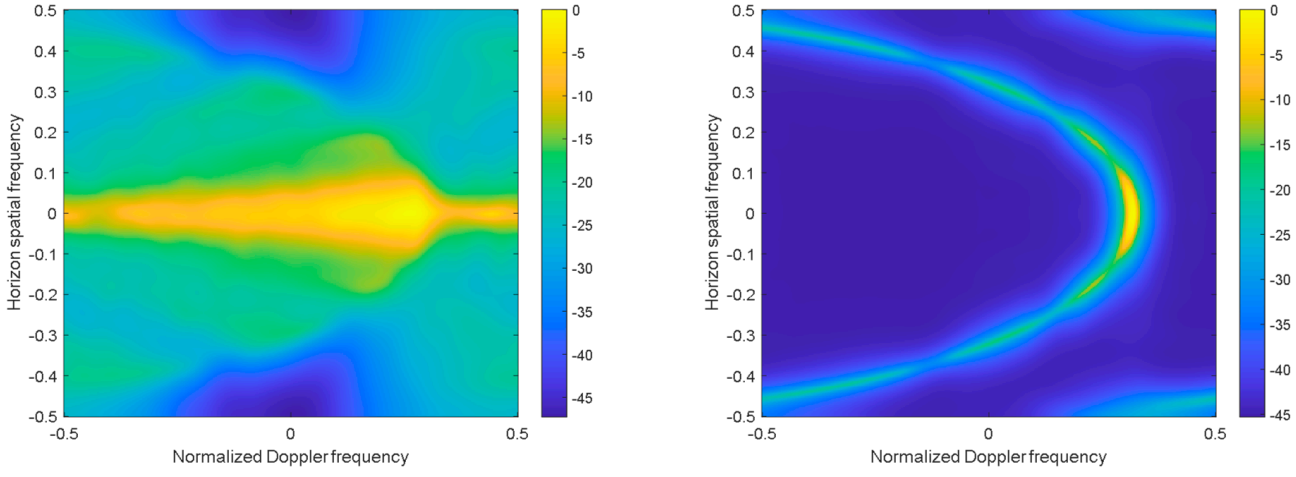

Figure 7. Separated clutter spectrum for the first and second range regions: (**a**) First range region; (**b**) Second range region.

4.4. Performance Analysis

In this part, the improved factor (IF) curve with respect to the normalized Doppler frequency is studied for clutter suppression performance evaluation. The IF is defined as the ratio of the output signal-to-clutter-plus-noise ratio (SCNR) to the input SCNR measured as a given element [1]. Figure 8 shows the IF curves corresponding to the four range regions. Due to the severe range dependency problem of the clutter from first range

region as shown in Figure 7a, the IF performance of STAP degrades dramatically. Nevertheless, clutter compensation can be performed since the range ambiguous problem has been alleviated. It is seen that the IF performance can be well maintained after clutter compensation. For the second, third, and fourth range regions, the IID condition is approximately satisfied; thus, STAP can be implemented with slight performance degradation. Therefore, the IF performance is improved after the range ambiguous clutter separation with the proposed method.

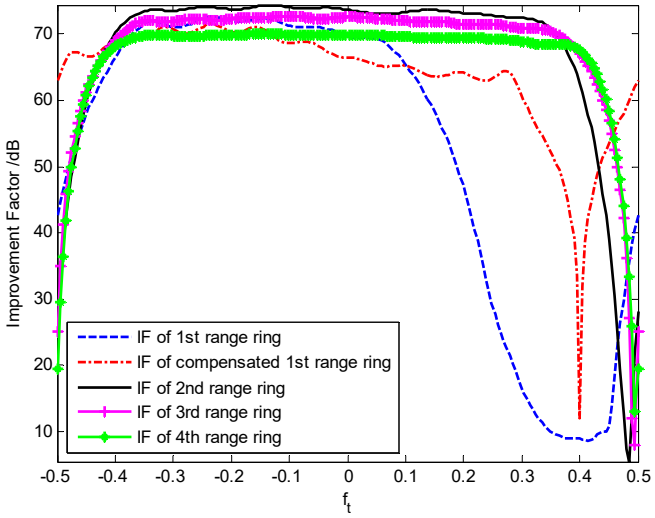

Figure 8. IF performance with respect to normalized Doppler frequency.

5. Conclusions

In this paper, a per-STAP beamforming method is devised for the vertical-FDA radar system to handle the range ambiguous echoes separation issue in the MPRF mode. In the proposed pre-STAP beamforming method, the advantages of frequency diversity and the additional DOFs in the range dimension are utilized to extract the echo of desired range region and to suppress echoes of ambiguous range regions, provided the prior knowledge of platform and radar parameters. To overcome the possible parameter uncertainty, an enhanced beamformer is presented by performing covariance matrix tapering. Thus, the enhanced per-STAP beamformer can be designed with specific properties—such as depth and width of the notch, shape of the main lobe, and so on. It is verified by the simulation results that the notches can be widened to improve the clutter suppression performance. As the beamformer is designed for each particular range, the computational complexity is increased. Nevertheless, it can be implemented in real-time because the pre-STAP beamformer can be constructed before collecting the radar echo. Moreover, another advantage of the pre-STAP beamformer is that the required element number in elevation can be sufficiently reduced without loss of performance.

Author Contributions: The contribution of authors is stated as follows: methodology and formulation, W.W. and J.X.; software realization, W.W. and J.X.; validation and experiments, P.W., J.Z., Z.L.; writing and review, W.W. and J.X. All authors have read and agreed to the published version of the manuscript.

Funding: This research was funded in part by Nature Science Foundation of China under grant numbers 61931016, 62071344, and 61911530246, in part by Key Laboratory Equipment Advanced Research Fund under grant number 6142206200210. The APC was funded by Nature Science Foundation of China.

Conflicts of Interest: The authors declare no conflict of interest.

References

1. Melvin, W.L. A STAP Overview. *IEEE Aerosp. Electron. Syst. Mag.* **2004**, *19*, 19–35. [CrossRef]
2. Cerutti-Maori, D.; Sikaneta, I. A Generalization of DPCA Processing for Multichannel SAR/GMTI Radars. *IEEE Trans. Geosci. Remote Sens.* **2013**, *5*, 560–572. [CrossRef]
3. Hale, T.B.; Temple, M.A.; Raquet, J.F.; Oxley, M.E.; Wicks, M.C. Localised three-dimensional adaptive spatial-temporal processing for airborne radar. *IEEE Proc. Radar Sonar Navig.* **2003**, *150*, 18–22. [CrossRef]
4. Fertig, L.B.; Krich, S.I. Benefits of 3d-stap for x-band GMTI airborne radars. In *2005 Adaptive Sensor Array Processing (ASAP) Workshop*; Lincoln Lab: Lexington, MA, USA, 2005.
5. Cui, N.; Duan, K.; Xing, K.; Yu, Z. Beam-space reduced-dimension 3D-STAP for nonside-looking airborne radar. *IEEE Geosci. Remote Sens. Lett.* **2015**, 1–5. [CrossRef]
6. Duan, K.; Xu, H.; Yuan, H.; Xie, H.; Wang, Y. Reduced-DOF three-dimensional STAP via subarray synthesis for nonsidelooking planar array airborne radar. *IEEE Trans. Aerosp. Electron. Syst.* **2020**, *56*, 3311–3325. [CrossRef]
7. Meng, X.; Wang, T.; Wu, J.; Bao, Z. Short-range clutter suppression for airborne radar by utilizing prefiltering in elevation. *IEEE Geosci. Remote Sens. Lett.* **2009**, *6*, 268–272. [CrossRef]
8. Wang, W. Frequency diverse array antenna: New Opportunities. *IEEE Antennas Propag. Mag.* **2015**, *57*, 145–152. [CrossRef]
9. Antonik, P.; Wicks, M.C.; Griffiths, H.D.; Baker, C.J. Multi-Mission Multi-Mode Waveform Diversity. In Proceedings of the 2006 IEEE Radar Conference, Verona, NY, USA, 24–27 April 2006; p. 3. [CrossRef]
10. Basit, A.; Wang, W.-Q.; Nusenu, S.Y.; Zhang, S. Range-angle-dependent beampattern synthesis with null depth control for joint radar communication. *IEEE Antennas Wirel. Propag. Lett.* **2019**, *18*, 1741–1745. [CrossRef]
11. Corbell, P.M.; Temple, M.A.; Hale, T.B. Forward-looking radar GMTI benefits using a linear frequency diverse array. *Electron. Lett.* **2006**, *42*, 1311–1312. [CrossRef]
12. Sammartino, P.F.; Baker, C.J.; Griffiths, H.D. Frequency Diverse MIMO Techniques for Radar. *IEEE Trans. Aerosp. Electron. Syst.* **2013**, *49*, 201–222. [CrossRef]
13. Xu, J.; Liao, G.; Zhu, S.; Huang, L.; So, H.C. Joint range and angle estimation using MIMO radar with frequency diverse array. *IEEE Trans. Signal Process.* **2015**, *63*, 3396–3410. [CrossRef]
14. Ding, Z.; Xie, J. Joint transmit and receive beamforming for cognitive FDA-MIMO radar with moving target. *IEEE Sens. J.* **2021**, *21*, 20878–20885. [CrossRef]
15. Xu, J.; Zhu, S.; Liao, G. Range ambiguous clutter suppression for airborne FDA-STAP radar. *IEEE J. Sel. Top. Signal Process.* **2015**, *9*, 1620–1631. [CrossRef]
16. Xu, J.; Liao, G.; So, H.C. Space-Time Adaptive Processing With Vertical Frequency Diverse Array for Range-Ambiguous Clutter Suppression. *IEEE Trans. Geosci. Remote Sens.* **2016**, *54*, 5352–5364. [CrossRef]
17. Xu, J.; Liao, G.; Zhang, Y.; Ji, H.; Huang, L. An adaptive range-angle-Doppler processing approach for FDA-MIMO radar using three-dimensional localization. *IEEE J. Sel. Top. Signal Process.* **2017**, *11*, 309–320. [CrossRef]
18. He, X.; Liao, G.; Zhu, S.; Xu, J.; Zhu, J.; Wang, C. An adaptive coding-angle-Doppler clutter suppression approach with extended azimuth phase coding array. *Signal Process.* **2020**, *169*, 107377. [CrossRef]
19. Yan, Y.; Wang, W.-Q.; Zhang, S.; Cai, J. Range-ambiguous clutter characteristics in airborne FDA radar. *Signal Process.* **2020**, *170*, 107407. [CrossRef]
20. Wen, C.; Peng, J.; Zhou, Y.; Wu, J. Enhanced three-dimensional joint domain localized STAP for airborne FDA-MIMO radar under dense false-target jamming scenario. *IEEE Sens. J.* **2018**, *18*, 4154–4166. [CrossRef]
21. Zatman, M. Comments on 'Theory and application of covariance matrix tapers for robust adaptive beamforming'. *IEEE Trans. Signal Process.* **2000**, *48*, 1796–1800. [CrossRef]
22. Mailloux, R.J. Covariance matrix augmentation to produce adaptive array pattern troughs. *IEEE Electron. Lett.* **1995**, *31*, 771–772. [CrossRef]
23. Zatman, M.A. Production of adaptive array troughs by dispersion synthesis. *IEEE Electron. Lett.* **1995**, *31*, 2141–2142. [CrossRef]
24. Guerci, J.R. Theory and application of covariance matrix tapers for robust adaptive beamforming. *IEEE Trans. Signal Process.* **1999**, *47*, 977–985. [CrossRef]